

SU(N) spin-wave theory: Application to spin-orbital Mott insulators

Zhao-Yang Dong, Wei Wang, and Jian-Xin Li*

National Laboratory of Solid State Microstructures and Department of Physics, Nanjing University, Nanjing 210093, China and Collaborative Innovation Center of Advanced Microstructures, Nanjing University, Nanjing 210093, China

(Dated: November 21, 2017)

We present the application of the SU(N) ($N > 2$) spin-wave theory to spin-orbital Mott insulators whose ground states exhibit magnetic orders. When taking both the spin and orbital degrees of freedom into account rather than projecting onto the Kramers doublet, the lowest spin-orbital locking energy levels, due to the inevitable spin-orbital multipole exchange interactions, the SU(N) spin-wave theory should take the place of the SU(2) one. To implement the application, we introduce an efficient general local mean field approach which involves all the local fluctuations into the SU(N) linear spin-wave theory. Our approach is tested firstly by calculating the multipolar spin-wave spectra of the SU(4) antiferromagnetic model. Then we apply it to spin-orbital Mott insulators. It is revealed that the Hund's coupling would influence the effectiveness of the isospin-1/2 representation when the spin orbital coupling is not large enough. Besides, we also calculate the spin-wave spectra based on the first principle calculations for two concrete materials, α -RuCl₃ and Sr₂IrO₄. The SU(N) spin-wave theory appropriately depicts the low-energy magnons and the spin-orbital excitations qualitatively.

I. INTRODUCTION

The physics of transition-metal oxides (TMOs) with 4d or 5d orbitals occupied has drawn considerable attention recently. One reason is that the spin-orbital coupling (SOC), which was considered as a small perturbation until recently, entangles the spin and orbital degrees of freedom. This effect in cooperation with electronic correlations could give rise to a novel type of insulators (spin-orbital Mott insulators) in which the local moments are spin-orbital entangled $J_{\text{eff}} = 1/2$ Kramers doublets¹⁻³. Another is their crystal structures with a special bond geometry formed by edge-shared octahedra, which will result in the anisotropy and the frustration of the effective Hamiltonian⁴, because the exchange coupling between the local moments depends highly on the spatial direction of the exchange path. The Hamiltonian with such a novel symmetry could lead to unconventional magnetism, including spin liquids, multipolar orders and uncommon magnetic orders¹. In real materials, the zigzag (Na₂IrO₃⁵ and 4d TMOs α -RuCl₃⁶⁻⁸), spiral (Li₂IrO₃⁹⁻¹¹) type magnetic orderings, and a canted antiferromagnetic (AF) structure (Sr₂IrO₄)^{12,13} have been proved.

Generally, 4d and 5d states are spatially so extended that the Hubbard interaction is reduced compared to that of 3d states. However, owing to the large crystal field and SOC, a separate band with a reduced bandwidth allows for the opening of a Mott gap. The underlying picture for this process is as following. For a d^5 electronic configuration, when the two e_g orbitals split off due to the crystal field of octahedrons, the five electrons loaded on the t_{2g} orbitals results in a $s = 1/2$ hole residing in an effective $l = 1$ orbitals. A strong SOC leads to a system with a fully filled $J_{\text{eff}} = 3/2$ band and a half-filled $J_{\text{eff}} = 1/2$ band. Thus, the so-called spin-orbital Mott insulators emerge even with a relatively small electronic correlation. In this case, the $J_{\text{eff}} = 1/2$ states present

the essential physics and effectively behavior as spin-1/2 pseudo spins. The resulting spin-exchange model can be obtained by projecting the electronic Hamiltonian onto the $J_{\text{eff}} = 1/2$ Kramers doublet which consists of only dipole-dipole interaction terms. To study the low-energy excitations of this spin-1/2 system with a magnetically ordered ground state, one can resort to the famous SU(2) linear spin-wave theory¹⁴. However, in many real materials the mixing between the e_g and t_{2g} orbitals are always presented and the deviation from the spherical symmetry drags some composition of $J_{\text{eff}} = 3/2$ states into the Kramers doublet¹⁵. In addition, the Hund's coupling in the multi-orbital system will induce electrons to orbit in the same direction. All of these would weaken the validity of the picture of a half-filling $J_{\text{eff}} = 1/2$ Kramers doublet, and complicate the spin exchange Hamiltonian by introducing the interactions between spin-orbital multipolar momentum¹. Thus, the spin-orbital multipolar orders and excitations are needed to be considered.

Generally, to study a spin-1/2 system with a magnetically ordered ground state and small quantum fluctuations, the famous SU(2) linear spin-wave theory¹⁴ are used, in which the spins are regarded as a classical three-components vector and its fluctuations are described by rotations of the vector. However, when the degrees of freedom of both spins and orbitals are involved, it is insufficient to treat the local states as the rotations of a classical three-components angular momentum. Therefore, a generalization of the SU(2) linear spin-wave theory is needed¹⁶. Recently, the SU(N) spin-wave theory based on the multi-boson approach has been introduced¹⁷⁻²⁰. Since the generators of the SU(N) group can be represented as bilinear forms in N -flavored bosons, instead of two bosons in the SU(2) spin-wave theory, the low-energy modes of the SU(N) spin-wave theory are described with $N - 1$ different bosons, which would provide a more accurate description of the low-energy excitations for unconventional magnetic orders.

In this paper, we will use the $SU(N)$ spin-wave theory to study the magnetic excitations in spin-orbital Mott insulators. In the $SU(N)$ spin-wave theory, the local order parameter is defined in the space of $SU(N)$ unitary transformations of the local spin states, instead of the $SU(2)$ space of local spin rotations, and it consists of $N^2 - 1$ components of the $SU(N)$ order parameter in the most general form. Therefore, a universal local mean field theory facilitating the $SU(N)$ spin-wave theory is required. Here, we introduce a general efficient local mean field theory based on the supercoherent state²¹, which fully includes the on-site quantum fluctuations essential for multipolar states. As an illustration, we first apply the $SU(N)$ spin-wave theory to a toy three-band Hubbard model on a hexagon lattice, and focus on the examination of the effect of Hund's coupling by calculating the weights of $J_{\text{eff}} = 1/2$ states in the ground state and spin-wave spectra. If the SOC is not large enough to lift the spin-orbital excitations across the $J_{\text{eff}} = 1/2$ and $J_{\text{eff}} = 3/2$ states away from those within the $J_{\text{eff}} = 1/2$ doublets, the Hund's coupling will compel the angular momentum L to parallel the spin momentum. Therefore, the low energy physics is not governed only by the $J_{\text{eff}} = 1/2$ effective Hamiltonian. We then study the spin excitations in two systems of TMOs, $\alpha\text{-RuCl}_3$ and Sr_2IrO_4 where the effective Hamiltonian include both spin and orbital degrees of freedom, by using the $SU(N)$ linear spin-wave theory. Our results for the magnetic ground states and their low-energy spin dynamics in two systems are consistent with recent experiments^{3,7,8,13}. In addition, we can obtain the high-energy spin-orbital excitations across the gap in the presence of the spin-orbital coupling.

The paper is organized in the following manner. In section II, we briefly review the Schwinger bosons representation and $SU(N)$ spin-wave theory, then introduce the general local mean field theory. In section III, based on the $SU(4)$ antiferromagnetic Hamiltonian²²⁻²⁴, we calculate its magnon excitations and spin-3/2's $l = 2$ multipole-multipole correlation function. In section IV, we apply the $SU(N)$ spin-wave theory to spin-orbital Mott insulators. First, we derive an effective Hamiltonian from a three-band Hubbard model with the SOC in the hexagon lattice and study the magnetic dynamics by the $SU(N)$ spin-wave theory. Then we calculate the spin correlation function of $\alpha\text{-RuCl}_3$ with the five-band Hubbard model and correlation function of resonant inelastic X-Ray scattering (RIXS) operators²⁵ of Sr_2IrO_4 with a three-band Hubbard model.

II. $SU(N)$ LINEAR SPIN-WAVE THEORY

Muniz et al present a mathematical framework of the multi-boson approach to generalize the traditional spin-wave theory from $SU(2)$ to $SU(N)$ ²⁰. As we know, the effective exchange models from the electron models in the

strong interaction limit would always be written as

$$H_0 = J_{\mu\nu\mu'\nu'}^{rr'} S_r^{\mu\nu} S_{r'}^{\mu'\nu'} + h_{\mu\nu}^r S_r^{\mu\nu}, \quad (1)$$

where the repeated index $r, r', \mu, \nu, \mu', \nu'$ is summed up, and $S_r^{\mu\nu}$ are the generators of $SU(N)$ group, which obey the commutation relations

$$[S_r^{\mu\nu}, S_{r'}^{\mu'\nu'}] = \delta_{r,r'} (S_r^{\mu\nu'} \delta_{\mu'\nu} - S_r^{\mu'\nu} \delta_{\mu\nu'}). \quad (2)$$

Then, they can be represented by Schwinger bosons. In the spin-wave theory, one of the bosons will be condensed depending on a given magnetic order and the rest $N - 1$ different bosons will be used to describe the low-energy modes of systems. In this section, we will first review the multi-boson approach based on the Schwinger bosons representation. Then, a general local mean field theory will be introduced and applied to the $SU(N)$ linear spin-wave theory.

A. Schwinger bosons representation

It is often useful to map a spin model into a bosonic one, which may be easier to study since bosons have simple commutation relations. Also, the common magnons are bosonic excitations which are proper to be represented in bosonic language. In the Schwinger bosons representation, the $SU(N)$ generators are written as²⁶,

$$S_r^{\mu\nu} = b_r^{\mu\dagger} b_r^\nu, \quad (3)$$

$$\sum_{\mu=0}^{n-1} b_r^{\mu\dagger} b_r^\mu = n_b, \quad (4)$$

where $b_r^{\mu\dagger}$ and b_r^μ ($\mu = 0, 1, \dots, n-1$) are bosonic creation and annihilation operators on the local site r , respectively. Eq. (4) is a constraint on the bosonic operators in the physical space. n_b is the number of bosons on the local site, denoting the order of the irreducible representations of $SU(N)$ group. For the well known $SU(2)$ linear spin-wave theory, we set $n_b = 2S$. Here we use $n_b=1$ for simplicity. Thus, n_b indicates the dimensions of the local state and there is an one-to-one match between each boson and each local dimension. Furthermore, the space of local operators is a n^2 -dimensional linear space, which could be expanded on the basis of the identity and the $n^2 - 1$ generators of $SU(N)$ group. Correspondingly, the identity is the constraint Eq. (4) and $n^2 - 1$ generators are bilinear forms $b^{\mu\dagger} b^\nu$. So, any local operator can be expressed as a linear combination of bosonic bilinear forms.

To sum up, all local fluctuations are described by bosonic particle-hole forms $b^{\mu\dagger} b^\nu$. For instance, if there is a local spin $S = 3/2$, then local fluctuations can be expanded by the multipole expansion, which has $16 = (2S + 1)^2$ different scattering channels classified by the total spin of a pair of particle and hole.

$$M_{l,m} = \sum_{m_1} (-1)^{s_2+m-m_1} C_{m_1, m-m_1, m}^{s_1, s_2, l} b^{s_1, m_1\dagger} b^{s_2, m_1-m}, \quad (5)$$

where $C_{m_1, m-m_1, m}^{s_1, s_2, l}$ are Clebsch-Gordan coefficients, and $(s_1, m_1), (s_2, m-m_1)$ are the spin quantum numbers of the particle and hole, respectively. $M_{l, m}$ is multipole spin operators. $M_{l, m}$ is the identity when $l = 0$, the dipolar operators S_+, S_- and S_z when $l = 1$, and the quadrupolar and octupolar operators when $l = 2, 3$. There are totally $16 = \sum_{l=0}^3 2l+1$ multipole spin operators, which are equal to the dimensions of the space of local operators and can also be expanded by $SU(N)$ generators. Therefore, $SU(N)$ spin-wave theory based on this multi-boson approach includes all of bosonic multipolar excitations.

B. Local mean field theory

It is necessary to construct a general local mean field theory to utilize all advantages of the $SU(N)$ spin-wave theory. As we known, the parameter manifold of a n -dimensional (n -D) state is $(n-1)$ -D complex projective space $CP(n-1)$ when the overall phase is neglected. There are $n-1$ complex parameters, which are $2(n-1)$ real parameters. The local mean-field state should travel all over the space, so according to the supercoherent states constructed by Fatyga et al²¹, we assume the test local wave function to be generated from a unitary transformation acting on an given state,

$$|T\rangle_r = U(\mathbf{x}_r) b_r^{0\dagger} |0\rangle. \quad (6)$$

$U(\mathbf{x}_r)$ is the unitary transformation and $|0\rangle$ is the vacuum without any bosons:

$$U(\mathbf{x}_r) = \exp[i \sum_{\mu \neq 0} (x_r^{2\mu-1} (b_r^{0\dagger} b_r^\mu + b_r^{\mu\dagger} b_r^0) + x_r^{2\mu} (i b_r^{\mu\dagger} b_r^0 - i b_r^{0\dagger} b_r^\mu))], \quad (7)$$

$$|0\rangle = \underbrace{(0, 0, 0, \dots, 0)}_n^T, \quad (8)$$

where $\mathbf{x} \in \mathbb{R}^{2(n-1)}$, the $2(n-1)$ -D real space. Obviously, $U(\mathbf{x}_r)$ is particle conserved, so the test state complies with the constraint Eq. (4). It is arduous to find the minimum in such a plain space. Thus, we will utilize the structure of $CP(n-1)$ to convert the $\mathbf{x} \in \mathbb{R}^{2(n-1)}$ parameter space to the rotation space in the n -D complex space,

$$\begin{aligned} x^1 &= \theta_1 \cos(\theta_2) \cos(\phi_1), \\ x^2 &= \theta_1 \cos(\theta_2) \sin(\phi_1), \\ x^3 &= \theta_1 \sin(\theta_2) \cos(\theta_3) \cos(\phi_2), \\ x^4 &= \theta_1 \sin(\theta_2) \cos(\theta_3) \sin(\phi_2), \\ &\dots, \\ x^{2n-3} &= \theta_1 \sin(\theta_2) \dots \sin(\theta_{n-1}) \cos(\phi_{n-1}), \\ x^{2(n-1)} &= \theta_1 \sin(\theta_2) \dots \sin(\theta_{n-1}) \sin(\phi_{n-1}), \\ \theta_j &\in \{0, \pi\}, \phi_j \in \{0, 2\pi\}. \end{aligned}$$

When $n = 2$, it is the well known state of spin-1/2, $|T\rangle = (\cos(\theta_1), e^{i\phi_1} \sin(\theta_1))^T$, where (θ_1, ϕ_1) are Euler angles. It

corresponds to a rotation in 2-D complex space or 3-D real space.

The mean field ground state of the system is the direct product state of local wave function, $|G\rangle = \bigotimes_r |T\rangle_r$, which would minimize the energy of $\langle G|H|G\rangle$. Due to the translational symmetry of the ground state, generally only the magnetic cell is considered in the spin-wave theory.

C. $SU(N)$ Linear spin-wave approximation

It is known that the spin-wave approximation is based on the Holstein-Primakoff (HP) bosons which define the spin-deviation operators. Its generalization can be obtained by extending the HP representation from $SU(2)$ to $SU(N)$ ²⁰. To obtain the $SU(N)$ HP bosons, we should first determine the condensed boson which creates the local state minimizing the mean-field energy. According to the variational form of the mean field ground state introduced in the last subsection, the condensed boson is the one minimizing $\langle G|H|G\rangle$, with $|G\rangle = \prod_r \tilde{b}_r^{0\dagger} \bigotimes |0\rangle_r$. It is related to the Schwinger boson \mathbf{b}_r via the unitary transformation Eq. (7),

$$\tilde{b}_r^{0\dagger} = \sum_\mu U_{0\mu}(\mathbf{x}_r) b_r^{\mu\dagger}. \quad (9)$$

Namely, $\tilde{b}_r^{0\dagger}$ is the $\mu = 0$ component of $\tilde{\mathbf{b}}_r$, and the corresponding creation and annihilation operator are replaced by a number according to the constraint of Eq. (4),

$$\tilde{b}_r^{0\dagger} \simeq \tilde{b}_r^0 \simeq \sqrt{1 - \sum_{\mu=1}^{n-1} \tilde{b}_r^{\mu\dagger} \tilde{b}_r^\mu}. \quad (10)$$

Then, the $N-1$ bosons $\tilde{b}_r^{\mu \neq 0}$ become the HP bosons, which describe the spin waves originating from fluctuations around the ordered spin state created by the condensed boson $\tilde{b}_r^{0\dagger}$. Substituting Eq. (10) into the Hamiltonian Eq. (1) and retaining only the quadratic terms, we get,

$$\begin{aligned} H \simeq & \sum_{\langle r, r' \rangle} J_{0000}^{rr'} + (J_{\mu 0 \nu'}^{rr'} b_r^{\mu\dagger} b_{r'}^{\nu'} + J_{0 \nu 0 \nu'}^{r, r'} b_r^\nu b_{r'}^{\nu'} + H.c) \\ & + \sum_r h_{00}^r + h_{\mu' \nu'}^r b_r^{\mu'} b_{r'}^{\nu'} + \sum_{\langle r, r' \rangle} [(J_{\mu \nu 00}^{rr'} - J_{0000}^{rr'} \delta_{\mu \nu}) b_r^{\mu\dagger} b_{r'}^{\nu'} \\ & + (J_{00 \mu' \nu'}^{rr'} - J_{0000}^{rr'} \delta_{\mu' \nu'}) b_r^{\mu'} b_{r'}^{\nu'}], \end{aligned} \quad (11)$$

where the index $\mu, \nu, \mu', \nu' \neq 0$ and will be summed up when appear twice in a single term, and the tilde \sim on $J_{\mu \nu \mu' \nu'}^{rr'}$ and b_r^μ , which denotes the expressions after the unitary transformation that minimizes the mean field variational energy, is omitted for simplicity.

Now Eq. (11) is a free bosonic Hamiltonian and can be solved by performing the Fourier transformation,

$$b_k^\mu = \frac{1}{\sqrt{L}} \sum_r b_r^\mu e^{i\mathbf{k} \cdot \mathbf{r}}, \quad (12)$$

with L the lattice number of the system. It leads to,

$$H = \sum_k \psi_k^\dagger h(k) \psi_k, \\ \psi_k = (b_k^1, \dots, b_k^{M(n-1)}, b_{-k}^{1\dagger}, \dots, b_{-k}^{M(n-1)\dagger})^T, \quad (13)$$

where M is the size of magnetic cell. There are two diagonalization methods for a bosonic Hamiltonian as proposed by White²⁷ and Colpa²⁸. After diagonalization, we get the spin-wave dispersion $\epsilon_\mu(k)$ as expressed by,

$$H = \sum_{\mu=1}^{M(n-1)} \epsilon_\mu(k) \gamma_k^{\mu\dagger} \gamma_k^\mu, \\ \gamma_k^\mu = T_{\mu'}^\mu b_k^{\mu'}, \quad (14)$$

with $T_{\mu'}^\mu$ the element of the matrix used to diagonalize the Hamiltonian. As noted, the $SU(N)$ spin-wave theory includes not only the dipole-dipole correlations, but also the multipole-multipole correlations. In general, the correlation function of two $SU(N)$ generators can be written by,

$$S^{\mu\nu\mu'\nu'}(k, \omega) = \frac{1}{2M(n-1)} \int dt e^{-i\omega t} \\ \times \sum_{r,r'} e^{i\mathbf{k}\cdot(\mathbf{r}-\mathbf{r}')} \langle S_r^{\mu\nu} S_{r'}^{\mu'\nu'}(t) \rangle. \quad (15)$$

As same as the $SU(2)$ linear spin-wave theory, only the quadratic forms of the dynamical part of correlation functions are calculated. Therefore, the correlation function is expanded in $\langle b^{\mu\dagger} b^\mu \rangle$, which describes the probability to excite one of bosonic excitations. It is clear that there are $M(n-1)$ spin-wave modes.

III. $SU(4)$ ANTIFERROMAGNETISM

As an example, we first calculate the spin-wave spectrum for the $SU(4)$ antiferromagnetic model in a square lattice. The model can be generated from the generic one-band Hubbard model loaded with spin-3/2 fermions. Due to Pauli's exclusion principle, the wave functions of two on-site fermions have to be antisymmetric. The total spin of two on-site spin-3/2 fermions can only be either singlet ($S=0$) or quintet ($S=2$). So the effective model at quarter-filling will have only two exchange channels, and the spin singlet channel results in the $SU(4)$ antiferromagnetic Hamiltonian:

$$H = J \sum_{\langle i,j \rangle} \left[\sum_{1 \leq a < b \leq 5} \Gamma_i^{ab} \Gamma_j^{ab} - \sum_{a=1}^5 \Gamma_i^a \Gamma_j^a \right], \quad (16)$$

where Γ^a are Dirac matrices which form Clifford algebra, $\{\Gamma^a, \Gamma^b\} = 2\delta^{ab}$ and $\Gamma^{ab} = [\Gamma^a, \Gamma^b]/(2i)$. Specifically, the five Dirac matrices can be expressed as tensor products of two Pauli spin-1/2 matrices ($\sigma^\alpha, \tau^\beta$), or

represented by symmetric bilinear combinations of the components of a spin-3/2 operator, S^x, S^y, S^z :

$$\Gamma^1 = \sigma^z \tau^y = \frac{1}{\sqrt{3}} \{S^y, S^z\}, \\ \Gamma^2 = \sigma^z \tau^x = \frac{1}{\sqrt{3}} \{S^x, S^z\}, \\ \Gamma^3 = \sigma^y \tau^0 = \frac{1}{\sqrt{3}} \{S^x, S^y\}, \\ \Gamma^4 = \sigma^x \tau^0 = \frac{1}{\sqrt{3}} [(S^x)^2 - (S^y)^2], \\ \Gamma^5 = \sigma^z \tau^z = (S^z)^2 - \frac{5}{4}.$$

First of all, the spin exchange Hamiltonian stems from a $SU(2)$ symmetrical one-band Hubbard model with spin-3/2 fermions, so it has the genetic $SU(2)$ symmetry. Also, all 15 Gamma operators together span the $SU(4)$ algebra. Among them, the 10 Γ^{ab} operators are $SO(5)$ anti-symmetric tensors, while the five Γ^a are $SO(5)$ vectors. Thus the Hamiltonian Eq. (16) obviously possesses $SO(5)$ symmetry. Moreover it also has a hidden $SU(4)$ symmetry in the bipartite lattice²³. We can define a particle-hole transformation $b^\mu \rightarrow \mathcal{J} b^{\mu\dagger}$ with an antisymmetric matrix $\mathcal{J} = i\sigma^x \tau^y$. With this operation, the fundamental representation transforms to a conjugate representation where $\Gamma^{ab*} = \Gamma^{ab}$ and $\Gamma^{a*} = -\Gamma^a$. If transforming all B sublattices into the conjugate representation, then we have,

$$H = J \sum_{\langle i,j \rangle} \left[\sum_{1 \leq a < b \leq 5} \Gamma_i^{ab*} \Gamma_j^{ab} + \sum_{a=1}^5 \Gamma_i^{a*} \Gamma_j^a \right]. \quad (17)$$

One should note that Eq. (16) is invariant under $SU(4)$ rotations and conjugate rotations on sublattices A and B , respectively, rather than under uniform $SU(4)$ transformations.

In a square lattice, the $SU(4)$ linear spin wave theory shows a long-range Neel order which is consistent with the quantum Monte Carlo simulations²⁹. There are three local order parameters of $SU(4)$ Neel order in the square lattice: $(\Gamma^{12}, \Gamma^{34}, \Gamma^5) = ((-1)^{x+y} m, (-1)^{x+y} m, m)$. In the case of spin-3/2, they can be expanded in multipole orders as defined in Eq. (5):

$$\Gamma^{12} = \frac{2}{\sqrt{5}} (2M_{1,0} - M_{3,0}), \\ \Gamma^{34} = \frac{2}{\sqrt{5}} (M_{1,0} + 2M_{3,0}), \\ \Gamma^5 = 2M_{2,0}.$$

Therefore, we choose to calculate a quadrupolar-quadrupolar correlation function along high symmetry directions,

$$M_2(k, \omega) \propto \sum_{r,r'} e^{i\mathbf{k}\cdot(\mathbf{r}-\mathbf{r}')} \int dt e^{-i\omega t} \left\langle \sum_m M_{2,m}(\mathbf{r}) M_{2,m}^\dagger(\mathbf{r}, t) \right\rangle,$$

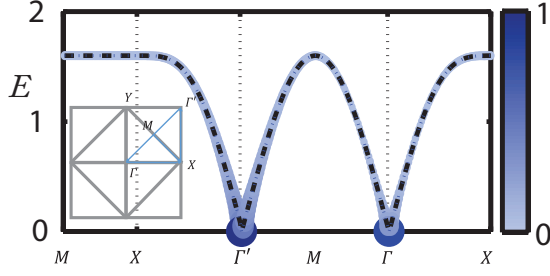


FIG. 1. (Color online) Spin waves of the SU(4) antiferromagnetic model in a square lattice along high symmetry directions. The dashed lines denote the dispersions, and the size and color of the marks indicate the intensity of the quadrupolar-quadrupolar correlation function.

The numerical results are shown in Fig. 1. The Goldstone manifold is $CP(3) = U(4)/[U(1) \otimes U(3)]$ with 6 branches of spin waves, which are degenerated and look like the dispersion of the SU(2) antiferromagnetic spin waves in a square lattice. However, the quadrupolar-quadrupolar correlation exhibits a noticeable intensity at the $\Gamma = (0, 0)$ point as shown in Fig. 1. It is in sharp contrast to the behavior of the antiferromagnetic spin-spin correlation, which vanishes at that point.

IV. SU(N) SPIN WAVE STUDY OF TMOS

As we know, most of TMOs have a magnetic ordered ground state. Considering that these magnetic ordered states can be described by isospins which are the entangled states of spin and orbital degrees of freedom, we use the SU(N) spin wave theory to investigate excitations from the ordered state. We will first present a general method to derive the effective exchange model from an electron model in the strong interaction limit. We consider the multi-band Hubbard model which is suitable to describe properties of TMOs,

$$H = \sum_{\langle ij \rangle, \alpha\alpha'} t_{\alpha\alpha'}^{ij} c_{i\alpha}^\dagger c_{j\alpha'} + \sum_i H_i.$$

Here the first term is hopping terms with $t_{\alpha\alpha'}^{ij}$ the element of hopping integrals, and α indicates all the local degrees of freedom, such as orbitals and spins. H_i are the local interactions which include the multi-band Hubbard term V_i , SOC O_i , and local potential field W_i ,

$$\begin{aligned} V_i = & \frac{1}{2} \sum_{mm'n'n'} \sum_{\sigma\tau\mu\nu} \delta_{\sigma\nu} \delta_{\tau\mu} \{ U \delta_{m=m'=n=n'} (1 - \delta_{\sigma\tau}) \\ & + U' \delta_{mn'} \delta_{m'n} (1 - \delta_{mm'}) + J_h \delta_{mn} \delta_{m'n'} (1 - \delta_{mm'}) \\ & + J' \delta_{mm'} \delta_{mn'} (1 - \delta_{mn}) (1 - \delta_{\sigma\tau}) \} \\ & \cdot c_{im\sigma}^\dagger c_{im'\tau}^\dagger c_{in\mu} c_{in'\nu}, \end{aligned} \quad (18)$$

$$O_i = \lambda \mathbf{S}_i \cdot \mathbf{L}_i, \quad (19)$$

$$W_i = \sum_{\alpha\beta} w_{i\alpha\beta} c_{i\alpha}^\dagger c_{i\beta}. \quad (20)$$

where U (U') is the intra-orbital (inter-orbital) Coulomb interaction, J_h and J' are the Hund's coupling and the pairing hopping, respectively. In this paper, we employ $U = U' + 2J_h$ and $J' = J_h$ as used usually.

By means of the perturbation theory, we treat the hopping terms as the perturbation in the strong interaction limit and obtain the effective exchange model which can be generally written as,

$$H_{\text{eff}} = \sum_i P_i^0 H_i P_i^0 + \sum_{\langle ij \rangle} [H_{i \rightarrow j} + H_{j \rightarrow i}], \quad (21)$$

$$H_{i \rightarrow j} = \sum_{\substack{(lre) \\ \alpha\alpha'\beta\beta}} \frac{1}{\Delta_{lre}} t_{\alpha'\alpha}^{\langle ij \rangle} [s_i^{\alpha'\beta'}]_{(lre)} t_{\beta\beta'}^{\langle ji \rangle} [\tilde{s}_j^{\beta\alpha}]_{(lre)} \quad (22)$$

The first term in Eq. (21) is the zero and first order perturbation term, and the second is the second order perturbation term accounting for the virtual hoppings of electrons contributing to spin exchanges. P_i^0 is the operator projecting the Hamiltonian H_i into its low-energy subspace. $s_i^{\alpha\beta} = c_{i\alpha}^\dagger c_{i\beta}$ and $\tilde{s}_i^{\beta\alpha} = c_{i\alpha} c_{i\beta}^\dagger$ are SU(N) generators and their conjugate representation, respectively. (lre) denotes various scattering channels related to the virtual processes from a low energy state $|\psi_r\rangle = \prod_i |r_i\rangle$ to a high one $|\psi_e\rangle = \prod_i |e_i\rangle$, and back to the low one $|\psi_l\rangle = \prod_i |l_i\rangle$, where $\prod_i |r_i\rangle$ is the eigenstate of Hamiltonian $\sum_i H_i$. $1/\Delta_{lre} = 1/2(E_{li} + E_{lj} - E_{ei} - E_{ej}) + 1/2(E_{ri} + E_{rj} - E_{ei} - E_{ej})$, in which E_{mi} ($m = l, e, r$) is the eigenenergy of the local state $|m_i\rangle$ on the site i . $[\]_{(lre)}$ indicates a special representation of $s_i^{\alpha\beta}$ and $\tilde{s}_j^{\beta\alpha}$ in the states $(|l_i\rangle, |r_i\rangle, |e_i\rangle)$

$$\begin{aligned} [s_i^{\alpha\beta}]_{(lre)} &= |l_i\rangle \langle l_i| c_i^{\alpha\dagger} |e_i\rangle \langle e_i| c_i^\beta |r_i\rangle \langle r_i|, \\ &= \langle l_i| c_i^{\alpha\dagger} |e_i\rangle \langle e_i| c_i^\beta |r_i\rangle S_i^{l_i r_i}, \\ [\tilde{s}_i^{\beta\alpha}]_{(lre)} &= |l_i\rangle \langle l_i| c_i^\alpha |e_i\rangle \langle e_i| c_i^{\beta\dagger} |r_i\rangle \langle r_i|, \\ &= \langle l_i| c_i^\alpha |e_i\rangle \langle e_i| c_i^{\beta\dagger} |r_i\rangle S_i^{l_i r_i}, \end{aligned}$$

where $S_i^{l_i r_i} = |l_i\rangle \langle r_i|$ is the SU(N) generator in the fundamental representation defined on the low-energy space of H_i . We note the symmetry of Hamiltonian Eq. (22) is related to the symmetry of $(|l_i\rangle, |r_i\rangle, |e_i\rangle)$ and $t_{\alpha'\alpha}^{ij}$, which are determined by the symmetry of the crystal structure. Now with Eq. (21), we will carry out the SU(N) spin wave calculation.

A. Three band Hubbard model with an SOC on the hexagon lattice

As an illustration of the application of the SU(N) spin wave theory, let us first consider a simple three band Hubbard model with one spin-1/2 particle per site and SOC, $-\lambda \vec{s} \cdot \vec{l}$ (The minus sign is due to that l is a mirror angular momentum) on the hexagon lattice. The Hubbard term

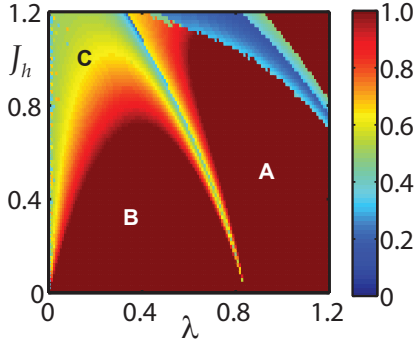


FIG. 2. (Color online) Weights of the $J_{\text{eff}} = 1/2$ states in ground states vary with λ and J_h , calculated based on the three band Hubbard model with an SOC on the hexagon lattice. The intra-orbital Coulomb interaction is $U = 5.0$

presents SU(2) and SO(3) symmetry with $U = U' + 2J_h$. Focusing on the effect of Hund's coupling and SOC, we suppose a simply isotropic hopping term, $t_{\alpha'\alpha}^{ij} = t\delta_{\alpha'\alpha}$ only among the nearest neighbours.

If SOC is absent, its effective exchange model is comparatively explicit. Because the wave functions of two on-site fermions have to be antisymmetric, there are only three exchange channels. The initial and final low energy states are singly occupied states with zero energy, and three intermediate states which are vacuum states on one site and doubly occupied states on the other site with 1) total spins are $S = 1$, total orbital momentums $L = 1$ and $\Delta_{lre} = -U + 3J_h$, 2) total spins are $S = 0$, total orbital momentums $L = 2$ and $\Delta_{lre} = -U + J_h$ and 3) total spins are $S = 0$, total orbital momentums $L = 0$ and $\Delta_{lre} = -U - 2J_h$. However, when SOC is comparable to the Hubbard term, $\lambda \sim U$, there will be $20 = 2 \times 5 \times 2$ channels due to the interplay of the SOC and Hund's coupling: two kinds of initial and final states with energy $\lambda/2$ and $-\lambda$ respectively, and five kinds of intermediate states with energy $U - 3J_h - \lambda/2$, $(2U - J_h - \lambda \pm \sqrt{25J_h^2 + 10J_h\lambda + 9\lambda^2})/2$ and $(4U - 8J_h + \lambda \pm \sqrt{16J_h^2 + 8J_h\lambda + 9\lambda^2})/4$. Substituting Δ_{lre} with the corresponding $(|l_i\rangle, |r_i\rangle, |e_i\rangle)$ and $t_{\alpha'\alpha}^{ij}$ into Eq. (22), we can easily obtain the exchange model numerically.

If $J_h = 0, \lambda = 0$, H_i has SU(6) symmetry, so does $(|l_i\rangle, |r_i\rangle, |e_i\rangle)$ and $t_{\alpha'\alpha}^{ij}$, but the symmetry of eigenstates will be broken into SU(2) by either SOC or Hund's coupling. Furthermore, when $t_{\alpha'\alpha}^{ij}$ is SU(2) symmetrical, the effective Hamiltonian must be SU(2) symmetrical too. If $\lambda \gg J_h$, only the lowest energy channel is active. In this case, the Hamiltonian can be further approximated to be an effective isospin-1/2 model. However, the Hund's coupling will lower the energy of the spin paralleling states of two electrons, while the SOC will lower the energy of single electron $J_{\text{eff}} = s - l = 1/2$ states. This would influence the validity of the isospin $J_{\text{eff}} = 1/2$ model. Therefore, we intend to take both λ and J_h into account to examine the SU(6) spin-wave spectrum of the system.

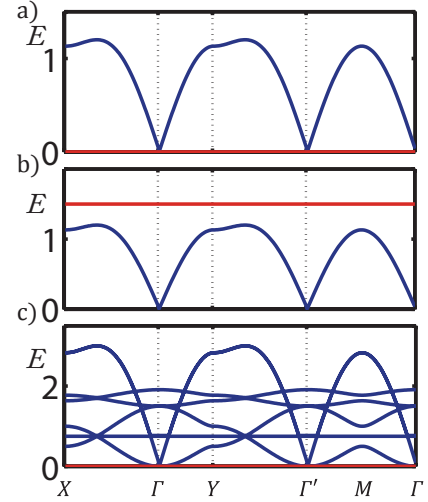


FIG. 3. (Color online) Spin waves of three band Hubbard model on the hexagon lattice with SOC λ and Hund's coupling J_h , which are: a) $\lambda = 0, J_h = 0$, b) $\lambda > 0, J_h = 0$ and c) $\lambda = 0, J_h > 0$.

Firstly, the local mean field theory suggests a magnetic cell with two sites, so we suppose the local mean field wave function in two sublattices of the hexagon lattice are $|T_A\rangle$ and $|T_B\rangle$. In order to verify the validity of the isospin $J_{\text{eff}} = 1/2$ model, we calculate the weight $(\langle J_{\text{eff}} = 1/2 | T_A \rangle + \langle J_{\text{eff}} = 1/2 | T_B \rangle) / 2$ of $J_{\text{eff}} = 1/2$ states in ground states as shown in Fig. 2. We use the hopping term $t = 1$ as unit, set $U = 5.0$ and change λ and J_h from 0 to 1.2. There are roughly three regions: **A**. Right-side region in which the ground states are dominated by $J_{\text{eff}} = 1/2$ states; **B**. A bump in the area of small λ and J_h where ground states are also dominated by $J_{\text{eff}} = 1/2$ states; **C**. J_h is so large that the ground states are mixed by the $J_{\text{eff}} = 3/2$ states. The blue discontinuous region on the right top is due to the divergence of the second order perturbation, which means the SOC gap is comparable to the Hubbard gap. Thus the low energy physics can certainly be described by the $J_{\text{eff}} = 1/2$ doublet in the region beyond this discontinuous region (where the SOC is dominated).

Let us first consider some extreme situations. The calculated dispersions for spin excitations in three band Hubbard model based on the spin wave theory for several cases are shown in Fig. 3. When $J_h = 0$ and $\lambda = 0$, there are highly degenerated zero energy spin waves suggesting that the magnetic order are unstable, as shown in Fig. 3 a). This is because the ground state is the SU(6) plaquette state^{30,31} in this situation, where SU(6) spins form local singlets on a hexagon plaquette. There is no long-range ordering on which the SU(N) spin wave theory is based, so the spin wave theory fails in this case. As λ increases, the zero energy spin waves are lifted [see Fig. 3 b)], and the system approaches ordered phases because the fluctuations become weak gradually as the system departs the SU(6) symmetry due to SOC. On the other

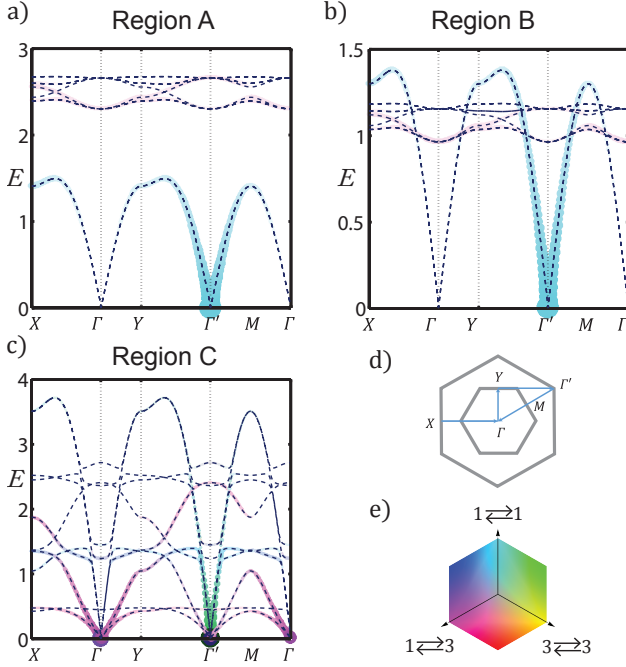


FIG. 4. (Color online) Spin waves with parameters: a) $\lambda = 0.9, J_h = 0.6$, b) $\lambda = 0.4, J_h = 0.4$ and c) $\lambda = 0.2, J_h = 1.1$. The dashed lines denote dispersions. The size and saturation of markers indicate the intensity of correlation function, and three different channels are indicated by three different colors. e) Reciprocal lattices and high symmetry directions of a hexagon lattice. d) The legend indicating the compositions of the correlation function.

hand, there is a ferromagnetic-like spin wave emerging when turning on the Hund's coupling J_h instead of SOC λ , as shown in Fig. 3 c). However, there is still some zero energy degeneracies. Thus, the ground state may be still an SU(6) plaquette state or some RVB states.

Then, we study the correlation functions in three regions **A**, **B** and **C**, respectively. In the dipole-dipole approximation, the correlation function consists of three parts of contributions: spin flippings within either $J_{\text{eff}} = 1/2$ or $3/2$ states and spin flippings across the $J_{\text{eff}} = 1/2$ and $J_{\text{eff}} = 3/2$ states, which are denoted by $1 \rightleftharpoons 1$, $3 \rightleftharpoons 3$ and $1 \rightleftharpoons 3$, respectively. In Figs 4 a)-c), we present the dispersions of spin waves denoted by the dashed lines and intensities of the correlation functions indicated by the saturation of three different colors and size of markers. The colors will mix as shown by the legend in Fig. 4 e), when spin wave excitations includes more than two types of contributions. In region **A**, the result suggests an antiferromagnetic-like spin wave at low energies, which is linear around Γ point and the intensity diverges at Γ' but vanishes at Γ point, and a ferromagnetic-like spin wave at high energies above 2, which is parabolic around Γ point and the intensity is higher at Γ than Γ' point. At the meantime, the result calculated by using the local mean field theory shows the system has a $J_{\text{eff}} = 1/2$ antiferromagnetic ordered ground state, confirming that the

excitations at low energies are indeed antiferromagnetic spin waves. As shown by the cyan-blue color in Fig. 4 a), these low-energy excitations comes basically from spin flippings within the $J_{\text{eff}} = 1/2$ states, so the low-energy physics in region **A** is dominated by isospin-1/2 states. Furthermore, the excitations arising from the spin flippings across the $J_{\text{eff}} = 1/2$ and $J_{\text{eff}} = 3/2$ states as denoted by the magenta color are far beyond the low-energy excitations due to the sufficiently large SOC. Thus, we arrive at the conclusion that an effective isospin Heisenberg model can depict the low-energy physics in region **A**, which is also consistent with the calculation of weights of $J_{\text{eff}} = 1/2$ states in ground states as shown in Fig. 2. When the SOC is decreased, we will enter gradually into region **B**. In this progress, the gap between the low-energy antiferromagnetic spin wave and the high-energy ferromagnetic spin wave decreases gradually. However, as long as J_h is not large enough, although the dispersion of ferromagnetic spin waves overlaps with the low energy one, the two spin waves do not entangle each other, as indicated by Fig. 4 b) where the colors representing two different kinds of spin waves do not mix. Thus, apart from the effective isospin Heisenberg terms in the Hamiltonian, which describes the antiferromagnetic spin waves, there have to be another term to describe the ferromagnetic spin waves at least. Starting from region **B**, one can increase J_h to enter into region **C**. In this region, the antiferromagnetic and ferromagnetic spin waves are entangled, so that there is no well-defined antiferromagnetic-like spin waves or ferromagnetic-like spin waves, and the local test wave functions of ground state in two different sublattices are not completely orthogonal, namely $\langle T_A | T_B \rangle \approx 0.016$. Because the ground state consists of both $J_{\text{eff}} = 1/2$ and $J_{\text{eff}} = 3/2$ states now, the multipolar orders are inevitable to be taken into account. Its dipolar order parameters $\langle J_{\text{eff}}^\alpha \rangle$ are almost antiferromagnetic, but quadrupolar order parameters $\langle J_{\text{eff}}^\alpha J_{\text{eff}}^\beta + J_{\text{eff}}^\beta J_{\text{eff}}^\alpha \rangle$ are ferromagnetic. In this case, all degrees of freedom have to be taken into account and there is no so-called isospin effective Hamiltonian, so the SU(N) spin wave theory rather than the traditional SU(2) one is applicable.

B. α -RuCl₃ and Sr₂IrO₄

In this subsection, we will use the SU(N) spin-wave theory to study spin dynamics in α -RuCl₃ and Sr₂IrO₄. Both α -RuCl₃ and Sr₂IrO₄ have a d^5 configuration and have an octahedral crystal field. Their differences are that the active electrons residing in $4d$ orbitals of Ru has a smaller SOC than that in $5d$ of Ir, and α -RuCl₃ is a honeycomb lattice while Sr₂IrO₄ is a square lattice.

α -RuCl₃ has a layered crystal structure with Ru³⁺ forming the honeycomb lattice layers and the energy bands near the Fermi level are dominated by the d orbitals of Ru. We consider a five band tight-binding model with five electrons per site and the on-site crystal fields to describe the $4d^5$ configuration of Ru³⁺. The tight-

binding parameters include the nearest-, next-nearest- and third-nearest-neighbour hopping integrals, which are obtained by fitting to the energy-band dispersions calculated by the first principle calculations and given in our previous paper Ref. [32]. We take $U = 2.7$ eV, $J_h = 0.13U$, $U' = U - 2J_h$, and $\lambda = 0.14$ eV^{7,15,32–35} in the following calculations. Then, an effective exchange model is obtained numerically according to Eq. (21). Due to the large crystal field potential on the e_g orbitals, there are isolated six lowest energy states, onto which we will project the initial and final states. Using the local mean field theory and the $SU(N)$ Linear spin-wave approximation introduced in Sec. II, we investigate numerically the magnetic ground state and spin dynamics. Numerical results show that the magnetic ground state has a zigzag type order of which the magnetic unit cell contains four sites (two cells), in agreement with experiments in α -RuCl₃^{6–8}. The spin-spin correlation functions calculated by Eq. (15) is shown in Fig. 5 a). Below 30 meV, four zigzag spin waves are evident, and the other sixteen excitations around 200 meV come from the spin-orbital excitations across the $J_{\text{eff}} = 1/2$ and $J_{\text{eff}} = 3/2$ states. Though there is long-range zigzag spin order, the results in Fig. 5 a) show that the low-energy spin waves have a gap of about 2 meV at M point and the spin-spin correlation function has a maximum magnitude also at M point. These results are consistent with the recent experiments of inelastic neutron scatterings on α -RuCl₃^{7,8}. On the other hand, the gap between the zigzag spin waves and the spin-orbital excitations is of about 210 meV, thus suggests that the low energy physics of α -RuCl₃ could be captured by an effective isospin-1/2 model. We have found in our previous paper Ref. [32] that the minimum effective isospin-1/2 model is the K- Γ model containing a ferromagnetic nearest-neighbor Kitaev interaction (K) and a nearest-neighbor off-diagonal exchange interaction (Γ).

Now let us turn to Sr₂IrO₄. We start our investigations from a three band Hubbard model with a single hole per site to fit the band dispersion around the Fermi level^{36,37}, and choose $U = 3.6$ eV, $J_h = 0.18U$, and $\lambda = 0.37$ eV in the calculation. Because iridium is a strong absorber of neutrons, it is more useful to calculate the resonant inelastic X-ray scattering (RIXS) spectrum for the purpose of a comparison with experiments. RIXS involves a second order process that includes an absorption and an emission of a photon. In the fast collision approximation, the direct RIXS spectrum is proportional to the correlation function of spin-orbital moment operators²⁵. Due to the two scattering progresses (absorption and emission), the total angular momentum of spin-orbital moment operators is equal to the coupling of two $l = 1$ angular momenta (angular momentum exchange of the two scatterings is one in the dipole limit). Thus, there exists multipole-multipole correlations in RIXS besides the usual dipole-dipole correlations. It is known that the RIXS spectrum of Sr₂IrO₄ is dependent on the incident angle³. So, we calculate the correlation function for

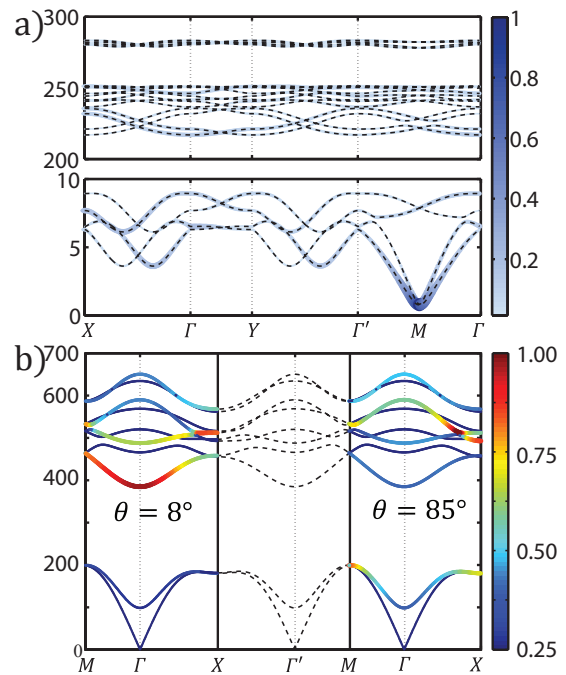


FIG. 5. (Color online) Spin-spin correlation functions for α -RuCl₃ a), and correlation functions of RIXS operators²⁵ for Sr₂IrO₄ b) along the high-symmetry lines, calculated by the $SU(N)$ spin-wave theory.

two different incident angles $\theta = 8^\circ, 85^\circ$ using the $SU(6)$ spin theory, and the results are presented in Fig. 5 b) where the left hand one is for $\theta = 8^\circ$ and right hand for $\theta = 85^\circ$. Below 200 meV, both results exhibit the gapless antiferromagnetic spin waves dispersing up linearly from the Γ point, which are consistent with experiments in Sr₂IrO₄^{3,12,13}. Above 200 meV, a gap of 180 meV exists arising from the SOC, and the spin-orbital excitations across the gap are ferromagnetic-like spin waves that are parabolic around Γ point. Moreover, there is a small gap in the spin-orbital exciton resulting from the splitting in the t_{2g} orbital. We also notice that these spin-orbital exciton modes correspond to a type of $SU(N)$ bosons in the framework of the $SU(N)$ spin-wave theory. As for the incident-angle dependence of the spectrum, one can see that the scattering intensity of the low-energy $J_{\text{eff}} = 1/2$ antiferromagnetic magnon is suppressed heavily, and at the same time the spin-orbital excitations are strongly enhanced for a small incident angle such as $\theta = 8^\circ$, as shown in the left-hand side in Fig. 5 b). While, an opposite behavior of the spectrum is observed for a large incident angle such as $\theta = 85^\circ$ (the right-hand side in Fig. 5 b)). Around the Γ' point, the intensity vanishes and only the dispersion of the spectrum is reserved, because the resolution is influenced due to the antiferromagnetic divergence at Γ' .

The results presented above demonstrate a good performance of the $SU(N)$ spin wave theory in the study of magnetic orders and dynamics in TMOs. Compared with the $SU(2)$ spin wave theory, the $SU(N)$ theory con-

tains more than one type of uncondensed bosons, so that the spin-orbital or multipolar orders and excitations can be captured. Of course, the linear approximation used here involves only single magnon excitations and does not take their interactions into account. So, the broadening and renormalization of the magnonic spectrum are not captured. To study other spin dynamics, such as magnon decay effects^{38,39}, one should go beyond the linear order approximation. We note that some modifications of the spin-wave theory^{40,41} have been developed in the SU(2) case, their generalizations to the SU(N) case deserve further study.

V. CONCLUSION

In summary, we implement the application of the SU(N) spin wave theory by introducing an efficient local mean field method based on the supercoherent state. The approach is tested firstly by applying to the investigation of magnetic properties in the SU(4) antiferromagnetic model in a square lattice. We find a long-range Neel order which is consistent with the quantum Monte Carlo simulations, and this order can be interpreted by multipolar orders of 3/2 spins. We have also calculated the multipolar spin waves of the SU(4) antiferromagnetic model, to demonstrate the application of SU(N) spin wave theory

in the description of multipolar orderings. Due to the entanglement of spin and orbital degrees of freedom, the multipole-multipole exchange terms are also present in the effective exchange models of spin-orbital Mott insulators. Only if the spin-orbital coupling is large enough that the low-energy physics is confined in Kramers doublet, the effective Hamiltonian will be described by an isospin-1/2 model. In this aspect, we examine a toy three-band Hubbard model on a hexagon lattice and find that the Hund's coupling also affects the validity of the isospin-1/2 picture when the spin-orbital coupling is below a critical value. Finally, we apply the SU(N) spin wave theory to two systems of spin-orbital Mott insulators, α -RuCl₃ and Sr₂IrO₄. Our results for the magnetic ground states and their low-energy spin dynamics in both systems are consistent with recent experiments. We also obtain the high-energy spin-orbital excitations across the gap in the presence of the spin-orbital coupling.

ACKNOWLEDGMENTS

This work was supported by the National Natural Science Foundation of China (11374138 and 11774152) and National Key Projects for Research and Development of China (Grant No. 2016YFA0300401).

-
- * jxli@nju.edu.cn
- ¹ W. Witczak-Krempa, G. Chen, Y. B. Kim, and L. Balents, *Annu. Rev. Condens. Matter Phys.* **5**, 57 (2014).
 - ² B. J. Kim, H. Jin, S. J. Moon, J.-Y. Kim, B.-G. Park, C. S. Leem, J. Yu, T. W. Noh, C. Kim, S.-J. Oh, J.-H. Park, V. Durairaj, G. Cao, and E. Rotenberg, *Phys. Rev. Lett.* **101**, 076402 (2008).
 - ³ J. Kim, M. Daghofer, A. H. Said, T. Gog, J. van den Brink, G. Khaliullin, and B. J. Kim, *Nat. Commun.* **5**, 4453 (2014).
 - ⁴ G. Jackeli and G. Khaliullin, *Phys. Rev. Lett.* **102**, 017205 (2009).
 - ⁵ X. Liu, T. Berlijn, W.-G. Yin, W. Ku, A. Tsvelik, Y.-J. Kim, H. Gretarsson, Y. Singh, P. Gegenwart, and J. P. Hill, *Phys. Rev. B* **83**, 220403 (2011).
 - ⁶ J. S. Sears, M. Songvilay, K. W. Plumb, J. P. Clancy, Y. Qiu, Y. Zhao, D. Parshall, and Y.-J. Kim, *Phys. Rev. B* **91**, 144420 (2015).
 - ⁷ A. Banerjee, J. Yan, J. Knolle, C. A. Bridges, M. B. Stone, M. D. Lumsden, D. G. Mandrus, D. A. Tennant, R. Moessner, and S. E. Nagler, *arXiv:1609.00103*.
 - ⁸ K. Ran, J. Wang, W. Wang, Z.-Y. Dong, X. Ren, S. Bao, S. Li, Z. Ma, Y. Gan, Y. Zhang, J. T. Park, G. Deng, S. Danilkin, S.-L. Yu, J.-X. Li, and J. Wen, *Phys. Rev. Lett.* **118**, 107203 (2017).
 - ⁹ A. Biffin, R. D. Johnson, I. Kimchi, R. Morris, A. Bombardi, J. G. Analytis, A. Vishwanath, and R. Coldea, *Phys. Rev. Lett.* **113**, 197201 (2014).
 - ¹⁰ S. C. Williams, R. D. Johnson, F. Freund, S. Choi, A. Jesche, I. Kimchi, S. Manni, A. Bombardi, P. Manuel, P. Gegenwart, and R. Coldea, *Phys. Rev. B* **93**, 195158 (2016).
 - ¹¹ A. Biffin, R. D. Johnson, S. Choi, F. Freund, S. Manni, A. Bombardi, P. Manuel, P. Gegenwart, and R. Coldea, *Phys. Rev. B* **90**, 205116 (2014).
 - ¹² B. J. Kim, H. Ohsumi, T. Komesu, S. Sakai, T. Morita, H. Takagi, and T. Arima, *Science* **323**, 1329 (2009).
 - ¹³ J. Kim, D. Casa, M. H. Upton, T. Gog, Y.-J. Kim, J. F. Mitchell, M. Van Veenendaal, M. Daghofer, J. Van Den Brink, G. Khaliullin, and B. J. Kim, *Phys. Rev. Lett.* **108**, 177003 (2012).
 - ¹⁴ J. T. Haraldsen and R. S. Fishman, *J. Phys.: Condens. Matter* **21**, 216001 (2009).
 - ¹⁵ H.-S. Kim, V. Shankar V., A. Catuneanu, and H.-Y. Kee, *Phys. Rev. B* **91**, 241110 (2015).
 - ¹⁶ A. Joshi, M. Ma, F. Mila, D. N. Shi, and F. C. Zhang, *Phys. Rev. B* **60**, 6584 (1999).
 - ¹⁷ B. Bauer, P. Corboz, A. M. Läuchli, L. Messio, K. Penc, M. Troyer, and F. Mila, *Phys. Rev. B* **85**, 125116 (2012).
 - ¹⁸ K. Penc, J. Romhányi, T. Röhm, U. Nagel, A. Antal, T. Fehér, A. Jánosy, H. Engelkamp, H. Murakawa, Y. Tokura, D. Szaller, S. Bordács, and I. Kézsmárki, *Phys. Rev. Lett.* **108**, 257203 (2012).
 - ¹⁹ J. Romhányi and K. Penc, *Phys. Rev. B* **86**, 174428 (2012).
 - ²⁰ R. A. Muniz, Y. Kato, and C. D. Batista, *Prog. Theor. Exp. Phys.* **2014**, 83I01 (2014).
 - ²¹ B. W. Fatyga, V. A. Kostecký, M. M. Nieto, and D. R. Truax, *Phys. Rev. D* **43**, 1403 (1991).
 - ²² Y. Qi and C. Xu, *Phys. Rev. B* **78**, 014410 (2008).

- ²³ C. Wu, J.-P. Hu, and S.-C. Zhang, Phys. Rev. Lett. **91**, 186402 (2003).
- ²⁴ H.-H. Hung, Y. Wang, and C. Wu, Phys. Rev. B **84**, 054406 (2011).
- ²⁵ J. Luo, G. Trammell, and J. Hannon, Phys. Rev. Lett. **71**, 287 (1993).
- ²⁶ D. P. Arovas and A. Auerbach, Phys. Rev. B **38**, 316 (1988).
- ²⁷ R. M. White, M. Sparks, and I. Ortenburger, Phys. Rev. **139**, A450 (1965).
- ²⁸ J. Colpa, Physica A **93**, 327 (1978).
- ²⁹ K. Harada, N. Kawashima, and M. Troyer, Phys. Rev. Lett. **90**, 117203 (2003).
- ³⁰ P. Nataf, M. Lajkó, P. Corboz, A. M. Läuchli, K. Penc, and F. Mila, Phys. Rev. B **93**, 201113 (2016).
- ³¹ H. H. Zhao, C. Xu, Q. N. Chen, Z. C. Wei, M. P. Qin, G. M. Zhang, and T. Xiang, Phys. Rev. B **85**, 134416 (2012).
- ³² W. Wang, Z.-Y. Dong, S.-L. Yu, and J.-X. Li, Phys. Rev. B **96**, 115103 (2017).
- ³³ A. Koitzsch, C. Habenicht, E. Müller, M. Knupfer, B. Büchner, H. C. Kandpal, J. van den Brink, D. Nowak, A. Isaeva, and T. Doert, Phys. Rev. Lett. **117**, 126403 (2016).
- ³⁴ L. J. Sandilands, Y. Tian, A. A. Reijnders, H.-S. Kim, K. W. Plumb, Y.-J. Kim, H.-Y. Kee, and K. S. Burch, Phys. Rev. B **93**, 075144 (2016).
- ³⁵ S. M. Winter, Y. Li, H. O. Jeschke, and R. Valentí, Phys. Rev. B **93**, 214431 (2016).
- ³⁶ H. Watanabe, T. Shirakawa, and S. Yunoki, Phys. Rev. Lett. **105**, 216410 (2010).
- ³⁷ H. Wang, S.-L. Yu, and J.-X. Li, Phys. Rev. B **91**, 165138 (2015).
- ³⁸ A. L. Chernyshev and M. E. Zhitomirsky, Phys. Rev. B **79**, 144416 (2009).
- ³⁹ S. M. Winter, K. Riedl, A. Honecker, and R. Valenti, arXiv:1702.08466.
- ⁴⁰ M. Takahashi, Phys. Rev. B **40**, 2494 (1989).
- ⁴¹ Z. Z. Du, H. M. Liu, Y. L. Xie, Q. H. Wang, and J.-M. Liu, Phys. Rev. B **92**, 214409 (2015).